Title
Yttrium-90 Portal Vein Radioembolization in Sprague-Dawley Rats: Dose-Dependent Imaging and Pathological Changes in Normal Liver.

Journal
Cardiovascular and interventional radiology, 43(12)

ISSN
0174-1551

Authors
Gordon, Andrew C
White, Sarah B
Gates, Vanessa L
et al.

Publication Date
2020-12-01

DOI
10.1007/s00270-020-02614-2

Peer reviewed

HHS Public Access

Author manuscript

Cardiovasc Intervent Radiol. Author manuscript; available in PMC 2021 December 01.

Published in final edited form as:

Cardiovasc Intervent Radiol. 2020 December ; 43(12): 1925–1935. doi:10.1007/s00270-020-02614-2.

Yttrium-90 Portal Vein Radioembolization in Sprague-Dawley Rats: Dose-dependent Imaging and Pathological Changes in Normal Liver

Andrew C. Gordon[1,2], **Sarah B. White**[3], **Vanessa L. Gates**[1], **Weiguo Li**[1], **Daniel Procissi**[1], **Zhuoli Zhang**[1], **Kathleen R. Harris**[1], **Dong-Hyun Kim**[1], **Samdeep K. Mouli**[1], **Reed A. Omary**[4], **Riad Salem**[1,5,6], **Andrew C. Larson**[1,2], **Robert J. Lewandowski**[1,5,6]

[1]Department of Radiology, Northwestern University Feinberg School of Medicine, Chicago, IL, USA

[2]Department of Biomedical Engineering, Northwestern University, Evanston, IL, USA

[3]Department of Radiology, Division of Vascular & Interventional Radiology, Medical College of Wisconsin, Milwaukee, WI, USA

[4]Department of Radiology and Radiological Sciences, Vanderbilt University, Nashville, TN, USA

[5]Department of Medicine-Hematology/Oncology, Northwestern University Feinberg School of Medicine, Chicago, IL, USA

[6]Department of Surgery-Organ Transplantation, Northwestern University Feinberg School of Medicine, Chicago, IL, USA

Abstract

PURPOSE—Portal vein embolization (PVE) is an established neoadjuvant method to induce future liver remnant hypertrophy prior to surgical resection of hepatic tumors. The purpose of our study was to examine the feasibility of PVE with glass ^{90}Y microspheres (Y90 PVE) in Sprague-Dawley rats. We tested the hypothesis that increased doses of Y90 PVE would increase target lobe fibrosis and atrophy.

METHODS—Twenty-two rats were assigned to four groups for Y90 PVE to the right median lobe: very high- (273.8MBq; n=2), high- (99.9MBq; n=10), medium- (48.1MBq; n=5), and low-dose (14.8MBq; n=5). An untreated control group included seven rats. ^{90}Y PET/CT of ^{90}Y distributions confirmed lobar targeting. MRI volumes were measured at baseline, 2-, 4-, 8- and 12-weeks. Explanted hepatic lobes were weighed, sectioned, and stained for H&E and immunohistochemistry. Digitized slides allowed quantitative measurements of fibrosis (20 foci/slide).

Corresponding Author: Robert J. Lewandowski, MD, Professor, Department of Radiology, Northwestern University Feinberg School of Medicine, 676 N. St. Clair, Suite 800, Chicago, IL 60611, : r-lewandowski@northwestern.edu.

Conflict of Interest: RAO and ACL are founders and owners of IO-RAD. RS and RJL are scientific advisors to BTG. RJL and ACG are consultants for ABK. SBW serves as a consultant for IO-RAD. None of the other authors have any conflict of interest.

Animal Subjects: All applicable international, national, and/or institution guidelines for the care and use of animals were followed.

Informed Consent: For this type of study, informed consent is not required.

Consent for Publication: For this type of study consent for publication is not required.

RESULTS—*Ex vivo* measurements confirmed 91–97% activity was localized to the target lobe (n=4). The percent growth of the target lobe relative to baseline was −5.0% (95% CI: −17.0–6.9%) for high-, medium dose rats compared to +18.6% (95% CI: +7.6–29.7%) in the low-dose group at 12-weeks (p=0.0043). Radiation fibrosis increased in a dose-dependent fashion. Fibrotic area/microsphere was 22,893.5, 14,946.2±2,253.3, 15,304.5±4,716.6, and 5,268.8±2,297.2μm^2 for very high- (n=1), high- (n=4), medium- (n=3), and low-dose groups (n=5), respectively.

CONCLUSION—Y90 PVE was feasible in the rat model, resulted in target lobe atrophy, and dose-dependent increases in hepatic fibrosis at 12 weeks. The onset of imaging-based volumetric changes was 8–12 weeks.

Keywords

portal vein embolization; hepatic radioembolization; magnetic resonance imaging; fibrosis; yttrium-90; dosing

INTRODUCTION

Portal vein embolization (PVE) is the current standard neoadjuvant approach to hypertrophy the future liver remnant (FLR) prior to surgical resection for primary and secondary hepatic malignancies [1–3]. The ideal embolic agent for PVE is unknown: particles, coils/plugs, and/or liquid embolic agents are all implemented. Up to 30% of patients do no convert to surgical resection, either because of insufficient FLR hypertrophy or due to tumor progression [4,5]. Therefore, new strategies are needed PVE for improved rates of FLR hypertrophy and antitumor activity. Some have advocated sequential transarterial chemoembolization followed by PVE (TACE+PVE) in effort to mitigate tumor progression prior to surgery in hepatocellular carcinoma (HCC) patients [6,7]. Even with this combination, progressive disease occurs in more than half of HCC patients and up to 28% do no convert to surgical resection [8].

Transarterial infusion of yttrium-90 microspheres (Y90), termed radiation lobectomy, is an alternative approach best described in HCC [9–11]. The use of PVE in patients with HCC and underlying cirrhosis/portal hypertension is controversial [12]; there is risk of worsening portal hypertension and/or promoting portal vein thrombosis as these are contraindications to PVE [13]. Radiation lobectomy has antitumor activity and also produces the desired atrophy-hypertrophy complex to facilitate resection. This approach may offer single-session treatment compared to TACE+PVE. A criticism of radiation lobectomy is delayed FLR hypertrophy in comparison to PVE [14]. Some favor this “test of time” prior to resection but more consistent methods for efficiently inducing FLR hypertrophy are needed.

We propose a new method of PVE with yttrium-90 microspheres (Y90 PVE) administered via the portal vein. The purpose of this study was to examine the feasibility of Y90 PVE. We hypothesized that target lobe fibrosis and atrophy would depend on the dose of ^{90}Y to the irradiated lobe.

MATERIALS AND METHODS

Study Design

Our institutional animal care and use committee approved this study, and all procedures were performed in accordance with ARRIVE guidelines. The use of glass ^{90}Y microspheres for research was approved and overseen by the Radiation Safety Officer of the university. A total of 32 male Sprague-Dawley rats (Charles River Laboratories, Wilmington, MA) weighing 450–500g were used for this study (Supplemental Figure 1). Twenty-two were treated with Y90 PVE. Each animal was assigned to one of four groups based on the planned ^{90}Y activity at infusion: very high- (273.8MBq; n=2), high- (99.9MBq; n=10), medium- (48.1MBq; n=5), and low-dose (14.8MBq; n=5). All procedures were performed with the intent of survival. Baseline and longitudinal MRI scans in survived rats provided anatomical assessments of hepatic volume changes. Liver specimens were harvested, weighed, and processed for histopathology and immunohistochemistry. An additional control group (n=7) included paired untreated rats ordered at the same time (similar weight and age), treated in the same environmental conditions, and terminated at the same 12-week study endpoint as Y90 PVE animals for hepatic lobar weight fractions, histopathology, and immunohistochemistry.

MR Imaging Protocols and Volumetry

T1-weighted and T2-weighted respiratory-gated imaging of the liver was accomplished at baseline, 2, 4, 8, and 12 weeks using a 7T 16-cm bore Bruker ClinScan MRI scanner (Bruker Biospin MRI GmbH, Ettlingen, Germany). Volumetric analyses included the total liver volume (TLV) and right median lobe (RML) volume in cm^3. On T2w images, the liver was manually contoured in the transverse view using hepatic and portal veins as anatomical landmarks. The hepatic veins were used to define four distinct hepatic lobes (right/left median, left lateral, right lateral, caudate). Volumetric analyses included the total liver volume (TLV) and right median lobe (RML) volume in cm^3. The RLL portal vein defined the inferior extent of the RML. The right portal and right hepatic veins defined the medial border with the lateral and superior borders defined by the liver capsule. The RML percent ratio was expressed as a percentage of the total liver volume and percent change in RML volume after Y90 PVE at n-weeks {n = 0, 2, 4, 8, 12} were defined as:

$$\text{RML \% ratio} = 100\% \times \text{RML} / \text{TLV}$$

$$\%\ \text{RML growth} = 100\% \times [\text{RML}_{\text{n weeks}} - \text{RML}_{\text{Baseline}}] / \text{RML}_{\text{Baseline}}$$

Additional details and pulse sequence parameters appear in the Supplemental Methods.

Portography and ^{90}Y Radioembolization

The abdomen was shaved and sterilely prepped with betadine scrub. A midline laparotomy was performed with externalization of the small bowel and an ileocolic venotomy was made with a 24½G angiocatheter (SURFLASH, Terumo Medical Co, Somerset, NJ). A

hydrophilic 0.018”, 80cm, angled Glidewire (Terumo Medical Co, Somerset, NJ) was passed through the angiocatheter under fluoroscopic guidance (OEC 9800 Plus mobile C-arm and vascular platform workstation, GE Medical Systems) to select the right portal vein, distal/central to the caudate portal veins in each case as variants in lobar portal venous supply in rats have been previously described [15]. The angiocatheter was exchanged for a 2Fr, 50cm JB1 angiocatheter (Cook Inc., Bloomington, Ind.) under fluoroscopic visualization and digital subtraction angiography (DSA) confirmed catheterization of the RML (Figure 1). Y90 PVE was performed by infusing 20–30μm glass ^{90}Y microspheres (TheraSphere®, BTG) in 6–8cc of sterile 0.9% saline over 1–2 minutes. Dose vials calibrated for 1GBq (9mg microspheres) were used in each animal and treatments occurred on days 5 (273.8MBq), 9 (99.9MBq), 12 (48.1MBq), and 16 (14.8MBq) post-calibration. Additional procedure details appear in the Supplemental Methods.

^{90}Y Dosimetry

After Y90 PVE, the delivered dose in Gy was calculated according to the Medical Internal Radiation Dose (MIRD) model using a calibrated Geiger-Mueller survey meter (Ludlum model 3, pancake probe model 44–9, Ludlum Measurements, Inc., Sweetwater, TX). Additional dosimetry details appear in the Supplemental Methods.

Ionization Chamber Measurements

The rats successfully infused that did not survive the procedure (n=4) were used to investigate biodistribution and validate ^{90}Y PET/CT imaging protocols via explanted tissues to measure the activity in the lungs and each hepatic lobe. The calibration number setting was based on a National Institute of Standards and Technology (NIST) report [16] and linearity was validated (R^2 = 0.999) with 30 measurements from ten dose vials containing glass ^{90}Y microspheres of known activities (standard error = 2.75 MBq) Supplemental Figure 2. Additional details appear in the Supplemental Methods.

^{90}Y PET/CT

A small animal PET/CT system (nanoScan, Mediso Medical Imaging Systems, Budapest, Hungary) was used for imaging ^{90}Y internal pair-production that allowed visualization of activity biodistributions and confirmation of RML targeting. A two-hour ^{90}Y PET imaging acquisition was completed *ex vivo* (n=4) and then *in vivo* (n=9) in survived rats. PET images were generated using Tera-Tomo 3D (1–5 detector coincidence) iterative ordered subset expectation maximization reconstruction on the ^{86}Y radionuclide setting with attenuation and scatter correction (4 iterations, 4 subsets, 212×212 matrix, 0.4mm slice thickness, 400–600keV energies). Dose vials (n=18) scanned at known activities were used to verify linearity and calibrate the scanner for the above protocol Supplemental Figure 3.

Necropsy & Histopathology

After completion of MR imaging at the 12-week study endpoint, all animals were euthanized and livers explanted. The right and left median lobes were separated along the median fissure and falciform ligament. Each hepatic lobe was weighed and specimens were embedded in a cryomold with O.C.T. compound (Sakura Finetek, Torrance, CA) and stored

at −80°C. The weight fraction for each lobe was calculated by normalizing the lobar weight by the total liver weight. Samples were sectioned en face with a slice thickness of 5μm. Consecutive slices were stained with hematoxylin and eosin (H&E) and Masson's trichrome for type IV collagen in fibrosis. The fibrotic area within each portal triad was manually contoured by analyzing 20 portal triads per slide (NanoZoomer, Hamamatsu Photonics).

Immunofluorescence

Sections of irradiated and non-irradiated liver were stained for immunofluorescence (IF) of hepatocyte proliferation with rabbit monoclonal anti-Ki67 (Abcam Inc., Cambridge, MA, USA), microvesseled density with rabbit anti-CD34 (Abnova, Atlanta, GA, USA), and stellate cell activation (α-SMA) was performed with mouse monoclonal anti-α-smooth muscle actin (DAKO Corp., Carpinteria, CA, USA). Digitized images were analyzed with ImageJ software (version 1.37, National Institutes of Health, Bethesda, MD). Additional IF details are included in the Supplemental Methods.

Statistical Analysis

All data were analyzed with the statistical package STATA (StataCorp, College Station, Texas). Data are reported as means ± standard deviation (SD) or medians with 95% confidence intervals (CI). Comparisons for two groups are evaluated by t test (normal distribution, means) and by Mann-Whitney *U* test (skewed distribution, medians). For three or more groups, analysis of variance (ANOVA) was used with Bonferonni correction. The medium to very high dose groups were combined and compared to the low dose group for liver volumetry changes as the low dose group represented the current clinical paradigm of 120 Gy liver dosing while the remaining groups represented varying degrees of escalated dosing. Analyses were considered statistically significant at *P*-values less than 0.05.

RESULTS

Y90 PVE

Three cases were attempted but aborted prior to radioembolization due to lengthy procedures or extravasation of contrast that would limit animal survival. Technically successful Y90 PVE was accomplished in 22 rats. ^{90}Y PET/CT was used to confirm delivery and four rats were excluded due to poor uptake in the target lobe and/or non-target delivery. The open laparotomy approach resulted in four immediate deaths after the procedure. Of the 18 rats that survived the Y90 PVE, 17/18 (94.4%) survived to the 12-week endpoint with one early death at four-week MRI. The mean fluoroscopy time (SD) was 2.8±1.7 min. Y90 dosing based on baseline MRI in the respective groups was: very high- (4621.7 Gy; n=1), high- (1406.0 ± 440.2 Gy; n=3), medium- (808.2 ± 82.5 Gy; n=2), and low-dose (156.8 ± 58.3 Gy; n=5).

^{90}Y PET/CT Dosimetry and Biodistribution

The mean calibrated vial activity was 0.93±0.17GBq. Median residual vial activity was 27.1%. Administered activity for each group is shown in Table 1. ^{90}Y PET/CT confirmed uptake in the target lobe in 9/13 cases (Figure 1) with poor uptake in the remaining cases

(Supplemental Figure 4). The relative percent activity in the lungs and each hepatic lobe in the four rats that did not survive the procedure are shown in Table 2.

MR Imaging

The volumetric changes in the target lobe (RML) appear in Figure 2. The onset of target lobe atrophy was 8–12 weeks for high- and medium-dose rats. The percent growth of the target lobe relative to baseline was −5.0% (95% CI: −17.0–6.9) for high-, medium dose rats compared to +18.6% (95% CI: 7.6–29.7) in the low-dose group (p=0.0043) at 12-weeks. The percentage of liver volume comprised of the target lobe was also decreased at 12-weeks for high/medium-dose rats at 11.4% (95% CI: 9.5–13.4) versus 15.1% (95% CI: 12.6–17.6) in low-dose rats (p=0.0120).

Explant Findings & Histology

Lobar mass increased as rats grew increasing whole liver and target lobe volume in both control and Y90 PVE groups. The weight fraction for each hepatic lobe appears in Figure 3. Medium- and high-dose Y90 PVE (but not low-dose) resulted in more extensive decreases in the target lobe weight fraction that was significantly less than the control group suggesting increased target lobe atrophy at these higher doses.

H&E demonstrated microspheres distributed throughout the portal triads in the target lobe (Figure 4). For the high-dose group, clusters of microspheres resulted in localized radiation necrosis and decellularization with residual extracellular matrix and peripheral fibrosis. The low-dose group demonstrated mild fibrosis within portal triads without necrosis or decellularization.

Areas of fibrosis were observed as dense circular regions of collagen deposition co-localized with microsphere distributions within the portal triads (shown in Figure 4) with sparring of the central veins. The fibrosis matched heterogeneous patterns of microsphere deposition within the hepatic parenchyma. The fibrotic area per microsphere was 22,893.5, 14,946.2±2,253.3, 15,304.5±4,716.6, and 5,268.8±2,297.2μm^2 for very high- (n=1), high- (n=4), medium- (n=3), and low-dose groups (n=5), respectively. Based on these values, radiation fibrosis extended to a mean circular radius of 85.4, 69.0±26.8, 69.8±38.7, and 50.0±27.0μm per sphere in each portal triad for each group, respectively. Fibrosis measurements are shown in Figure 5 by administered activity (MBq) and specific activity of infused microspheres (MBq/mg).

Immunofluorescence results are shown in Figure 6. Y90 PVE decreased hepatocyte proliferation in the target lobe for high- and medium-dose rats with 4.5 versus 16.1 Ki67 positive nuclei per field in the target versus non-target lobe, respectively (p=0.0061). For the very high-, high-, and medium-dose rats, microvessel density was significantly reduced in the target lobe at 544.6 (CI: 241.3–847.9) versus 2245.9 (CI: 1782.5–2709.4) per mm^2 in the non-target lobe (p=0.0001). The area of positive α-SMA staining in high-/medium-dose rats was similarl for the target and non-target lobe at 0.40% (CI: 0.16–0.65) versus 0.32% (CI: 0.02–0.62), respectively (p=0.3077).

One early death occurred at four-week imaging and was considered related to the duration of scanning rather than ^{90}Y because ^{90}Y PET/CT demonstrated no off-target delivery and this correlated with pathology in this case. Trichrome staining demonstrated extensive subcapsular fibrosis that matched gross pathology, indicating onset of fibrosis as early as one month after Y90 PVE (Supplemental Figure 5). Hepatocyte proliferation was also diminished in the target lobe compared to the non-target liver; however, the numbers of positive nuclei per field were higher compared those observes at 12-weeks suggesting increased growth rates at four-weeks compared to 12-weeks (in agreement with MRI volumetry data). Although the microvessel density was not decreased at this early time-point, microvessels in the target lobe appeared thickened and stained more densely in comparison to those in the non-target lobe, suggesting potential early changes in vascular dilatation and permeability in the target lobe.

DISCUSSION

Y90 PVE was feasible in Sprague-Dawley rats, resulting in increased target lobe atrophy at higher dosing levels. The onset of atrophy was 8–12 weeks. Fibrosis in portal triads was observed and extended from microspheres a radial distance of 50–85μm per sphere depending on dose. Fibrosis was observed as early as four weeks, and the extent of fibrosis at 12 weeks increased with increasing administered activity and increasing specific activity of infused microspheres. Treatment with ^{90}Y in the target lobe resulted in decreased hepatocyte proliferation and decreased density of sinusoidal endothelial cells relative to the non-target liver.

Toskitch et al. published a case report describing the use of trans-portal radioembolization as a salvage therapy in an HCC patient with hepatic arterial damage from prior chemoembolization procedures and systemic therapy [17]. This case demonstrated the clinical potential for Y90 PVE. Our study confirms induction of target lobe fibrosis and atrophy with ^{90}Y microspheres, termed Y90 PVE, a new concept for PVE with the intent of radioablative lobectomy. Current approaches for PVE include embolization with various combinations of embolic materials (coils/plugs, n-butyl cyanoacrylate, ethanol, ethiodized oil, fibrin glue, polyvinyl alcohol or trisacryl gelatin particles); however, the optimal technical approach is unknown as randomized studies comparing various agents are lacking, it is unclear what size particles, amount of embolic material, or angiographic endpoints are needed to achieve a specific degree or rate of FLR hypertrophy. A concern with all the above approaches is reflux of the embolic material into veins supplying the FLR due to risk of bilateral or main portal vein occlusion. Despite this risk, all tumor-bearing liver should be embolized due to the observed risk of accelerated tumor growth in non-embolized liver [18]. In contradistinction to the above approaches that do not provide direct antitumor activity, Y90 is a microembolic therapy that delivers high dose radiation to the tumor bed. Therefore, stasis or substasis angiographic endpoints were not used in our study and portal venous occlusion was not required to induce fibrosis/atrophy in the target lobe.

Y90 as the embolic agent for PVE could theoretically improve oncologic outcomes as HCC is known to spread through small portal vein radicles, and HCC may have increased blood supply from the portal vein after prior transarterial therapies [19,20]. Moreover, colorectal

liver metastases derive perfusion from the portal vein [21]. Thus, delivery of microembolic Y90 (20–30μm) into the portal veins and peripheral small radicles could limit tumor metastases, seeding during liver manipulation/mobilization, and allow treatment of tumors with increased perfusion from the portal vein. These oncologic aspects warrant further investigation.

Currently, intra-arterial delivery of Y90 for radiation lobectomy is an alternative method to induce FLR hypertrophy that also provides tumor control but has slower time to FLR hypertrophy than PVE [9–11]. We theorize the ideal clinical paradigm may be combining transarterial radioembolization with Y90 PVE to optimize oncologic outcomes and promoting faster rates of FLR hypertrophy. Combination approaches including TACE+PVE and PVE with hepatic venous embolization (venous deprivation technique) have recently been implemented to improve the outcomes for PVE [6–8,22,23].

A range of clinically relevant doses versus the conventional dose of 120Gy was implemented in our study because the requisite dose to induce target lobe atrophy from a transportal approach is unknown. Clinical data suggest significant target lobe atrophy may not be observed at 120Gy dosing [11]. This mirrors our finding that 150+Gy dosing did not arrest growth in the target lobe. Increased target lobe atrophy was observed in groups dosed at 800+ and 1400+Gy; however, the high and very high-dose groups did not have more extensive atrophy compared to the medium dose group, suggesting a threshold dose. Therefore, induction of the atrophy-hypertrophy complex for FLR augmentation may require doses higher than the conventional 120Gy.

Hepatic fibrosis at three months following radioembolization is evident by elastography [24]. This observation combined with the median time to resection of ~86–90d at our institution led us to select 12 weeks as an appropriate study endpoint for Y90 PVE in rats. Imaging findings after radioembolization have been previously reported by Miller et al. and reviewed by Bester et al. [25,26]. Our findings confirm fibrotic changes after hepatic radioembolization, previously indirectly imaged [27]. In addition, medium- and high-dose Y90 PVE reduced the density of sinusoidal endothelial cells in the target lobe, a promising finding if this effect translates to microvascular damage in a clinical setting.

This study was limited by lack of a tumor model. The rat model has been previously used to study tumor growth kinetics after PVE [28]. We applied an open surgical approach and survival after the open laparotomy for Y90 PVE improved with experience but in clinical practice PVE is performed with percutaneous techniques. Rats grew in size over the course of the study and the atrophy-hypertrophy complex remains to be demonstrated after Y90 PVE. Future studies could assess whether the Y90 PVE-induced target lobe atrophy and fibrosis translate to contralateral lobar hypertrophy and the rabbit model may be especially useful for these further investigations [29–31]. Meanwhile, additional work in the rodent model could allow for more rigorous examinations of dose-dependent toxicity to the normal liver tissue for example in the setting of radiosensitivity of the noncirrhotic parenchyma to Y90 chemoradiation [32].

CONCLUSION

Y90 PVE was feasible in the rodent model and resulted in target lobe atrophy and radiation fibrosis that increased with higher dosing. This approach warrants future study as a neoadjuvant therapeutic option with attention to oncologic outcomes and induction of the atrophy-hypertrophy complex.

Supplementary Material

Refer to Web version on PubMed Central for supplementary material.

Acknowledgements

The authors thank Northwestern University Healthy Physics (Jose Macatangay, Joseph Princewill, Thomas E. Whittenhall Jr., Angelica E. Gheen). Survival studies were supported through dedicated housing and accommodation by the Center for Comparative Medicine (Dr. Stephen I. Levin, Giovanni Pompilio). Imaging for our studies was made possible by Northwestern University's Center for Translational Imaging (Sol Misener).

Funding: We are grateful for the generous funding that supported this work provided by the SIR Foundation Allied Scientist Grant (ACG) and the Department of Radiology of the Feinberg School of Medicine. ACG Medical Scientist Training Program (T32GM008152). Dose vials, administration kits, and additional funding was provided through an Investigator Initiated Study (IIS) grant from BTG. RS is supported in part by NIH grant CA126809. SBW receives salary support from NIH 5R25 CA132822-03. Histology services were provided by the Northwestern University Mouse Histology and Phenotyping Laboratory which is supported by NCI P30-CA060553 and the Robert H Lurie Comprehensive Cancer Center Pathology Core Facility (Bernice Frederick, Adriana Rosca, Demirkan Gürsel).

ABREVIATIONS

ANOVA	analysis of variance
CE	contrast enhanced
CI	confidence interval
DSA	digital subtraction angiography
FLR	future liver remnant
GRE	gradient recalled echo
H&E	hematoxylin and eosin
ICL	inferior caudate lobe
IF	immunofluorescence
LLL	left lateral lobe
MIP	maximum intensity projection
MIRD	Medical Internal Radiation Dose
MRI	magnetic resonance imaging
PET/CT	positron emission tomography / computed tomography

PVE	portal vein embolization
RML	right median lobe
ROI	regions-of-interest
SCL	superior caudate lobe
T2W	T2-weighted MRI
TACE	transarterial chemoembolization
TSE	turbo spin echo
TLV	total liver volume
Y90	yttrium-90
Y90 PVE	yttrium-90 portal vein embolization

REFERENCES

[1]. Farges O, Belghiti J, Kianmanesh R, Regimbeau JM, Santoro R, Vilgrain V, et al. Portal vein embolization before right hepatectomy: prospective clinical trial. Ann Surg 2003;237:208–17. doi:10.1097/01.SLA.0000048447.16651.7B. [PubMed: 12560779]

[2]. Ribero D, Chun YS, Vauthey J-N. Standardized liver volumetry for portal vein embolization. Semin Intervent Radiol 2008;25:104–9. doi:10.1055/s-2008-1076681. [PubMed: 21326551]

[3]. Madoff DC, Abdalla EK, Vauthey J-N. Portal vein embolization in preparation for major hepatic resection: evolution of a new standard of care. Jvir 2005;16:779–90. doi:10.1097/01.RVI.0000159543.28222.73. [PubMed: 15947041]

[4]. Nagino M, Kamiya J, Nishio H, Ebata T, Arai T, Nimura Y. Two hundred forty consecutive portal vein embolizations before extended hepatectomy for biliary cancer: surgical outcome and long-term follow-up. Ann Surg 2006;243:364–72. doi:10.1097/01.sla.0000201482.11876.14. [PubMed: 16495702]

[5]. Ribero D, Abdalla EK, Madoff DC, Donadon M, Loyer EM, Vauthey JN. Portal vein embolization before major hepatectomy and its effects on regeneration, resectability and outcome. Br J Surg 2007;94:1386–94. doi:10.1002/bjs.5836. [PubMed: 17583900]

[6]. Yoo H, Kim JH, Ko G-Y, Kim KW, Gwon DI, Lee S-G, et al. Sequential transcatheter arterial chemoembolization and portal vein embolization versus portal vein embolization only before major hepatectomy for patients with hepatocellular carcinoma. Ann Surg Oncol 2011;18:1251–7. doi:10.1245/s10434-010-1423-3. [PubMed: 21069467]

[7]. Vilgrain V, Sibert A, Zappa M, Belghiti J. Sequential arterial and portal vein embolization in patients with cirrhosis and hepatocellular carcinoma: the hospital beaujon experience. Semin Intervent Radiol 2008;25:155–61. doi:10.1055/s-2008-1076689. [PubMed: 21326556]

[8]. Ronot M, Cauchy F, Gregoli B, Breguet R, Allaham W, Paradis V, et al. Sequential transarterial chemoembolization and portal vein embolization before resection is a valid oncological strategy for unilobar hepatocellular carcinoma regardless of the tumor burden. HPB (Oxford) 2016;18:684–90. doi:10.1016/j.hpb.2016.05.012. [PubMed: 27485063]

[9]. Gaba RC, Lewandowski RJ, Kulik LM, Riaz A, Ibrahim SM, Mulcahy MF, et al. Radiation Lobectomy: Preliminary Findings of Hepatic Volumetric Response to Lobar Yttrium-90 Radioembolization - Springer. Ann Surg Oncol 2009;16:1587–96. doi:10.1245/s10434-009-0454-0. [PubMed: 19357924]

[10]. Vouche M, Lewandowski RJ, Atassi R, Memon K, Gates VL, Ryu RK, et al. Radiation lobectomy: Time-dependent analysis of future liver remnant volume in unresectable liver cancer

as a bridge to resection. J Hepatol 2013;59:1029–36. doi:10.1016/j.jhep.2013.06.015. [PubMed: 23811303]

[11]. Lewandowski RJ, Donahue L, Chokechanachaisakul A, Kulik L, Mouli S, Caicedo J, et al. (90) Y radiation lobectomy: Outcomes following surgical resection in patients with hepatic tumors and small future liver remnant volumes. J Surg Oncol 2016. doi:10.1002/jso.24269.

[12]. May BJ, Madoff DC. Controversies of preoperative portal vein embolization. Hepatic Oncology 2016;3:155–66. doi:10.2217/hep-2015-0004. [PubMed: 30191035]

[13]. Madoff DC, Denys A, Wallace MJ, Murthy R, Gupta S, Pillsbury EP, et al. Splenic arterial interventions: anatomy, indications, technical considerations, and potential complications. Radiographics 2005;25 Suppl 1:S191–211. doi:10.1148/rg.25si055504. [PubMed: 16227491]

[14]. Garlipp B, de Baere T, Damm R, Irmscher R, Van Buskirk M, Stübs P, et al. Left-liver hypertrophy after therapeutic right-liver radioembolization is substantial but less than after portal vein embolization. Hepatology 2014;59:1864–73. doi:10.1002/hep.26947. [PubMed: 24259442]

[15]. Sänger C, Schenk A, Schwen LO, Wang L, Gremse F, Zafarnia S, et al. Intrahepatic Vascular Anatomy in Rats and Mice--Variations and Surgical Implications. PLoS ONE 2015;10:e0141798. doi:10.1371/journal.pone.0141798. [PubMed: 26618494]

[16]. Zimmerman BE, Cessna JT. Experimental determinations of commercial “dose calibrator” settings for nuclides used in nuclear medicine. Appl Radiat Isot 2000;52:615–9. [PubMed: 10724415]

[17]. Toskich BB, Tabriz DM, Zendejas I, Cabrera R, Geller B. Transportal Radioembolization as Salvage Hepatocellular Carcinoma Therapy to Maintain Liver Transplant Candidacy. J Vasc Interv Radiol 2015;26:1479–83. doi:10.1016/j.jvir.2015.06.029. [PubMed: 26408214]

[18]. Elias D, de Baère T, Roche A, Mducreux, Leclere J, Lasser P. During liver regeneration following right portal embolization the growth rate of liver metastases is more rapid than that of the liver parenchyma. Br J Surg 1999;86:784–8. doi:10.1046/j.1365-2168.1999.01154.x. [PubMed: 10383579]

[19]. Goseki N, Nosaka T, Endo M, Koike M. Nourishment of hepatocellular carcinoma cells through the portal blood flow with and without transcatheter arterial embolization. Cancer 1995;76:736–42. doi:10.1002/1097-0142(19950901)76:5<736::aid-cncr2820760505>3.0.co;2-q. [PubMed: 8625174]

[20]. Miyayama S, Matsui O, Yamashiro M, Ryu Y, Kaito K, Ozaki K, et al. Ultraselective transcatheter arterial chemoembolization with a 2-f tip microcatheter for small hepatocellular carcinomas: relationship between local tumor recurrence and visualization of the portal vein with iodized oil. J Vasc Interv Radiol 2007;18:365–76. doi:10.1016/j.jvir.2006.12.004. [PubMed: 17377182]

[21]. Ekelund L, Lin G, Jeppsson B. Blood supply of experimental liver tumors after intraarterial embolization with gelfoam powder and absolute ethanol. Cardiovasc Inter Rad 1984;7:234–9. doi:10.1007/bf02553141.

[22]. Guiu B, Chevallier P, Denys A, Delhom E, Pierredon-Foulongne M-A, Rouanet P, et al. Simultaneous trans-hepatic portal and hepatic vein embolization before major hepatectomy: the liver venous deprivation technique. Eur Radiol 2016;26:4259–67. doi:10.1007/s00330-016-4291-9. [PubMed: 27090112]

[23]. Guiu B, Quenet F, Escal L, Bibeau F, Piron L, Rouanet P, et al. Extended liver venous deprivation before major hepatectomy induces marked and very rapid increase in future liver remnant function. Eur Radiol 2017;27:3343–52. doi:10.1007/s00330-017-4744-9. [PubMed: 28101681]

[24]. Bas A, Samanci C, Gulsen F, Cantasdemir M, Kabasakal L, Kantarci F, et al. Evaluation of Liver Stiffness After Radioembolization by Real-Time ShearWave™ Elastography: Preliminary Study. Cardiovasc Inter Rad 2014. doi:10.1007/s00270-014-1021-z.

[25]. Miller FH, Keppke AL, Reddy D, Huang J, Jin J, Mulcahy MF, et al. Response of liver metastases after treatment with yttrium-90 microspheres: role of size, necrosis, and PET. Multiple Values Selected 2007;188:776–83. doi:10.2214/AJR.06.0707.

[26]. Bester L, Hobbins PG, Wang S-C, Salem R. Imaging characteristics following 90yttrium microsphere treatment for unresectable liver cancer. J Med Imaging Radiat Oncol 2011;55:111–8. doi:10.1111/j.1754-9485.2011.02241.x. [PubMed: 21501398]

[27]. Jakobs TF, Saleem S, Atassi B, Reda E, Lewandowski RJ, Yaghmai V, et al. Fibrosis, portal hypertension, and hepatic volume changes induced by intra-arterial radiotherapy with 90yttrium microspheres. Dig Dis Sci 2008;53:2556–63. doi:10.1007/s10620-007-0148-z. [PubMed: 18231857]

[28]. Bretagnol F, Maggiori L, Zappa M, Sibert A, Vilgrain V, Panis Y. Selective portal vein embolization and colorectal liver metastases in rat: a new experimental model for tumor growth study. J Surg Res 2011;171:669–74. doi:10.1016/j.jss.2010.03.047. [PubMed: 20605581]

[29]. de Graaf W, van den Esschert JW, van Lienden KP, Roelofs JJTH, van Gulik TM. A rabbit model for selective portal vein embolization. J Surg Res 2011;171:486–94. doi:10.1016/j.jss.2010.04.032. [PubMed: 20691990]

[30]. Hoekstra LT, van Lienden KP, Verheij J, van der Loos CM, Heger M, van Gulik TM. Enhanced tumor growth after portal vein embolization in a rabbit tumor model. J Surg Res 2013;180:89–96. doi:10.1016/j.jss.2012.10.032. [PubMed: 23149224]

[31]. Páramo M, García-Barquin P, Santa María E, Madrid JM, Caballeros M, Benito A, et al. Evaluation of the rabbit liver by direct portography and contrast-enhanced computed tomography: anatomical variations of the portal system and hepatic volume quantification. Eur Radiol Exp 2017;1:7. doi:10.1186/s41747-017-0011-8. [PubMed: 29708175]

[32]. Hickey R, Mulcahy MF, Lewandowski RJ, Gates VL, Vouche M, Habib A, et al. Chemoradiation of hepatic malignancies: prospective, phase 1 study of full-dose capecitabine with escalating doses of yttrium-90 radioembolization. Int J Radiat Oncol Biol Phys 2014;88:1025–31. doi:10.1016/j.ijrobp.2013.12.040. [PubMed: 24661655]

Synopsis

Transportal radioembolization in Sprague-Dawley rats induces dose-dependent fibrosis and decreased volume in the target lobe at 8–12 weeks.

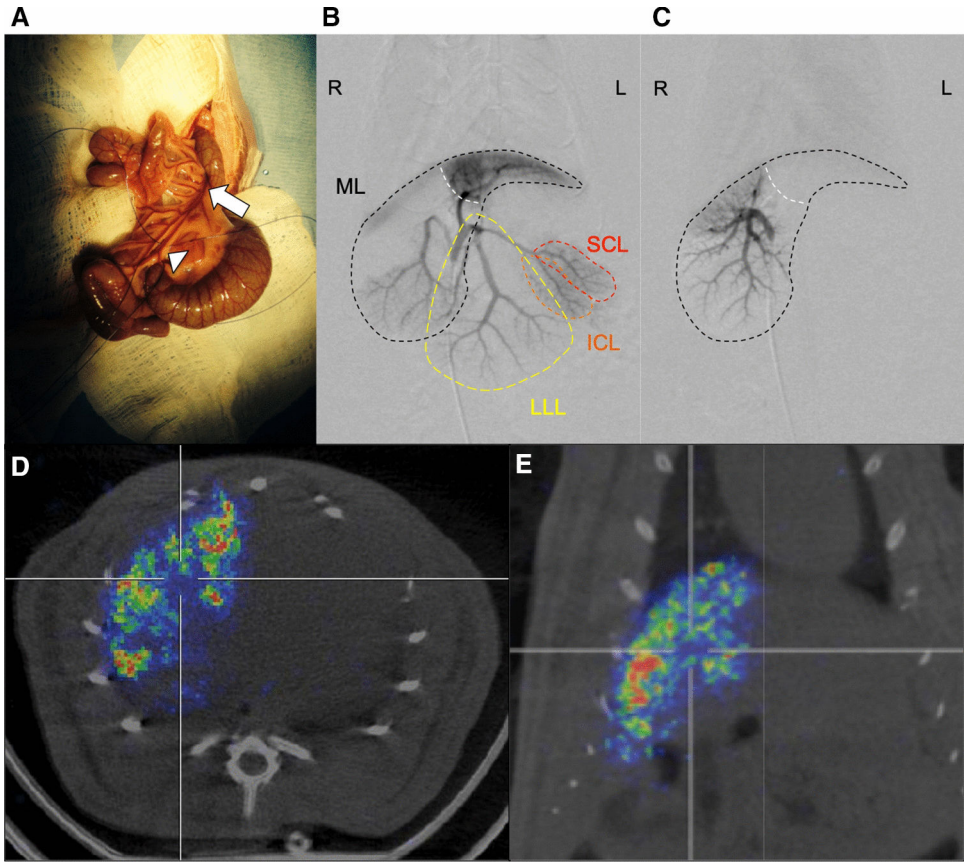

Figure 1.

(A) Externalization of bowel reveals mesenteric vein (arrow), tributaries, and site for venupuncture (arrowhead) with suture placement above and below. (B) DSA portogram with catheter tip positioning in the main portal vein demonstrates preferential flow and parenchymal opacification of the left segment of the median lobe (ML), left lateral lobe (LLL), superior caudate lobe (SCL), and inferior caudate lobe (ICL). The white dashed line delineates margin between irradiated and non-irradiated tissue. Note that the right lateral lobe (RLL) is not observed in this image. (C) Transcatheter selection of the right portal vein provides improved visualization of the right median lobe without reflux into the left portal vein or retrograde flow to the gastrointestinal tract. Y90 PVE was performed with this catheter tip positioning for selective delivery to the right median lobe. (D) Immediate post-procedure ^{90}Y PET/CT demonstrates right median lobe (RML) activity distributions in axial and (E) coronal fused images.

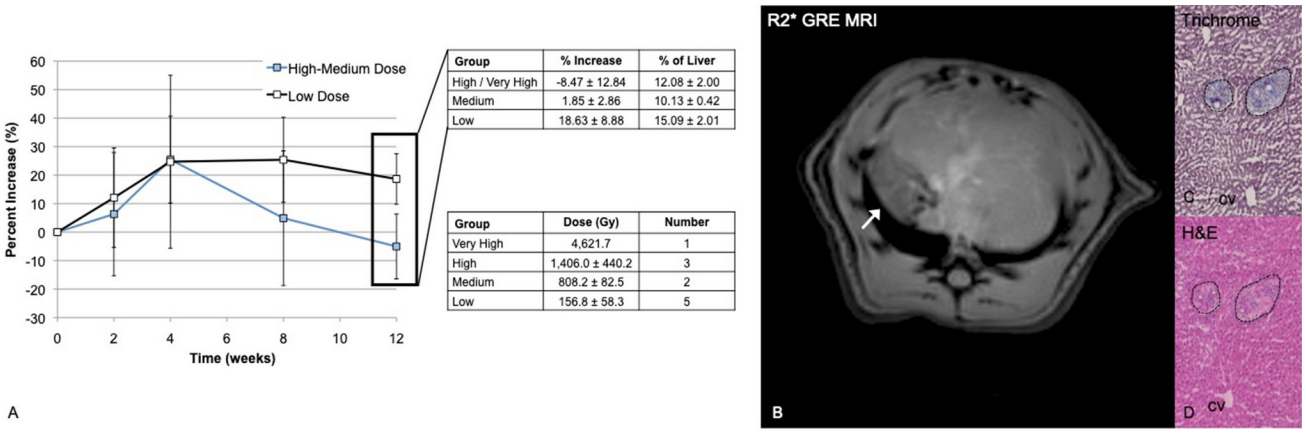

Group	% Increase	% of Liver
High / Very High	-8.47 ± 12.84	12.08 ± 2.00
Medium	1.85 ± 2.86	10.13 ± 0.42
Low	18.63 ± 8.88	15.09 ± 2.01

Group	Dose (Gy)	Number
Very High	4,621.7	1
High	1,406.0 ± 440.2	3
Medium	808.2 ± 82.5	2
Low	156.8 ± 58.3	5

Figure 2.

(A) MRI volumetry after Y90 PVE (n=11). After 12 weeks, the relative increase in RML volume from baseline was −8.5%, 1.9%, and 18.6% for the high/very high-, medium-, and low-dose groups, respectively. Values are reported as means ± SD. (B) Radiation changes included decreased signal and atrophy in the target RML on follow-up R2* GRE MRI. Histopathology with (C) Masson's trichrome staining showed fibrosis (outlined) with (D) corresponding H&E sections confirming fibrosis within portal triads with sparing of the central veins (cv = central vein).

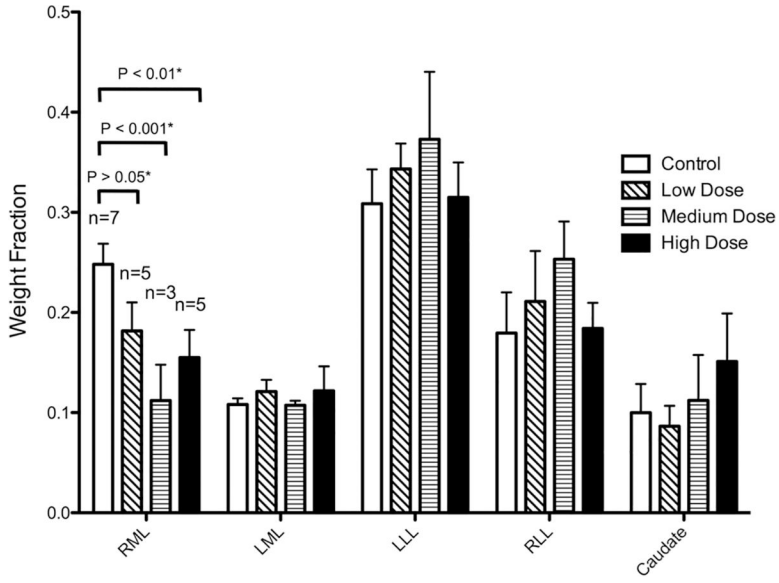

Figure 3.

Hepatic lobar weight fractions by dose group at 12 weeks post Y90 PVE. Two-way ANOVA with Bonferroni corrected p-values (*). In comparison to controls, medium- and high-dose groups had significant reductions in target lobe (RML) hepatic weight fractions while the low-dose group did not.

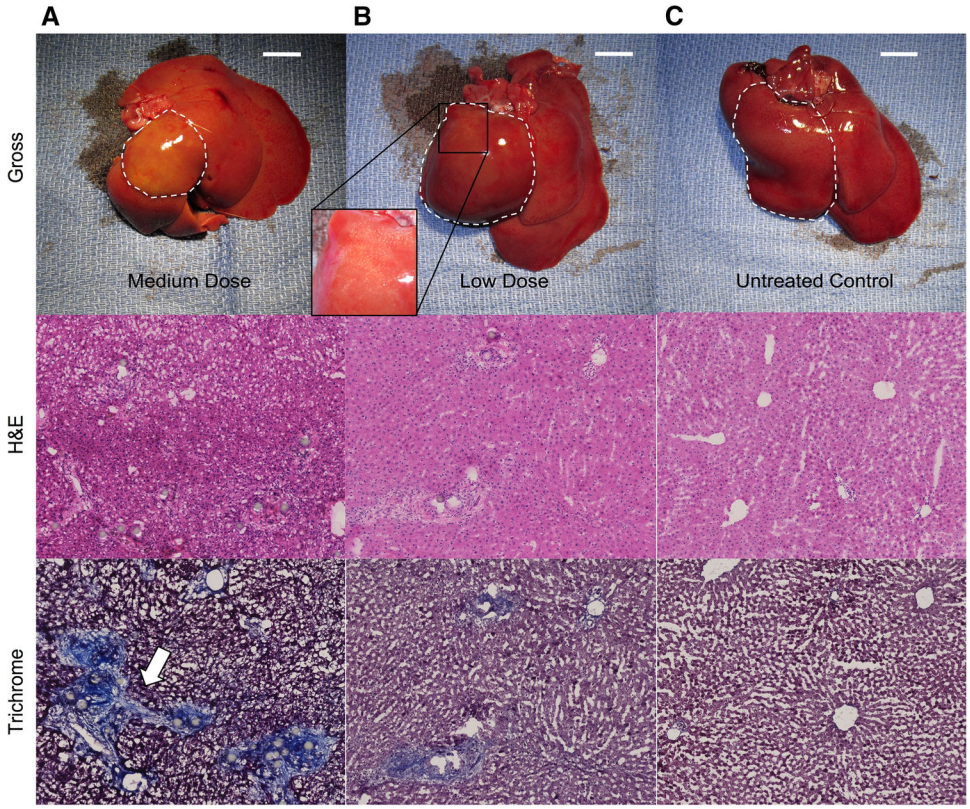

Figure 4.

Gross pathology of explanted livers 12 weeks following Y90 PVE. (A) Medium dose infusion resulted in marked atrophy of the irradiated RML (outlined). The ratio of RML to LML volume clearly reverses in this case (RML < LML). (B) The low dose group demonstrated little to no atrophy of the RML, and the size of this lobe exceeded that of the LML as in the case of untreated controls. Qualitatively, low dose infusions resulted in a finely granulated “sandpaper” appearance of the capsular surface (inset) with an otherwise similar morphology and texture in comparison to the (C) untreated controls. Scale bar = 1cm. Histopathology at 100x optical magnification of the RML after (A) medium-dose infusion, (B) low-dose infusion, and (C) no infusion (controls). (A) The areas of fibrosis overlay with microsphere distributions throughout the target lobe. Medium dose Y90 PVE resulted in significant fibrosis (blue) within the irradiated RML; these areas of fibrosis were restricted to short distances around heterogeneous clusters of microspheres throughout the parenchyma with bridging fibrosis (arrows) joining portal triads and sparing of the central veins. (B) The low dose group demonstrated mild fibrosis of the treated RML. (C) Untreated controls showed no fibrosis.

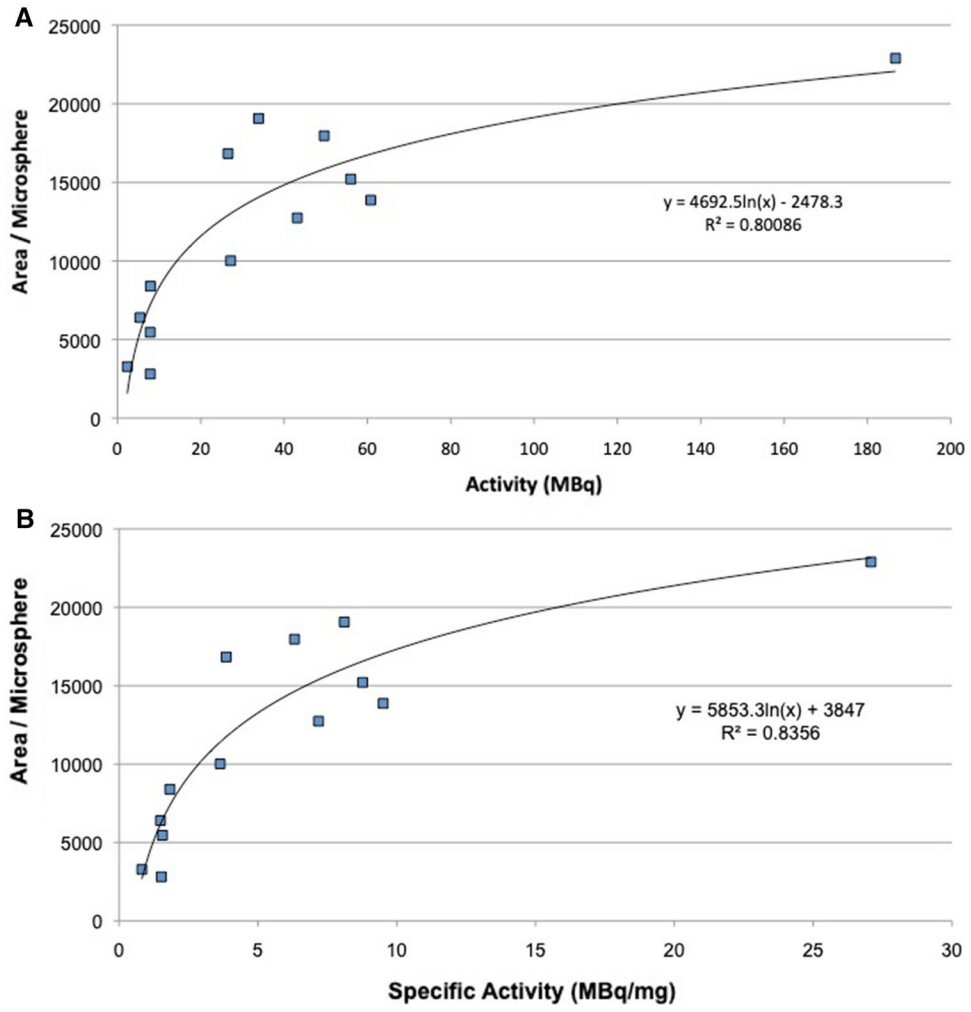

Figure 5.

Fibrosis measurements. The fibrotic area (μm^2) per microsphere within portal triads increased with increased (A) administered activity (MBq) and (B) increased specific activity (MBq/mg).

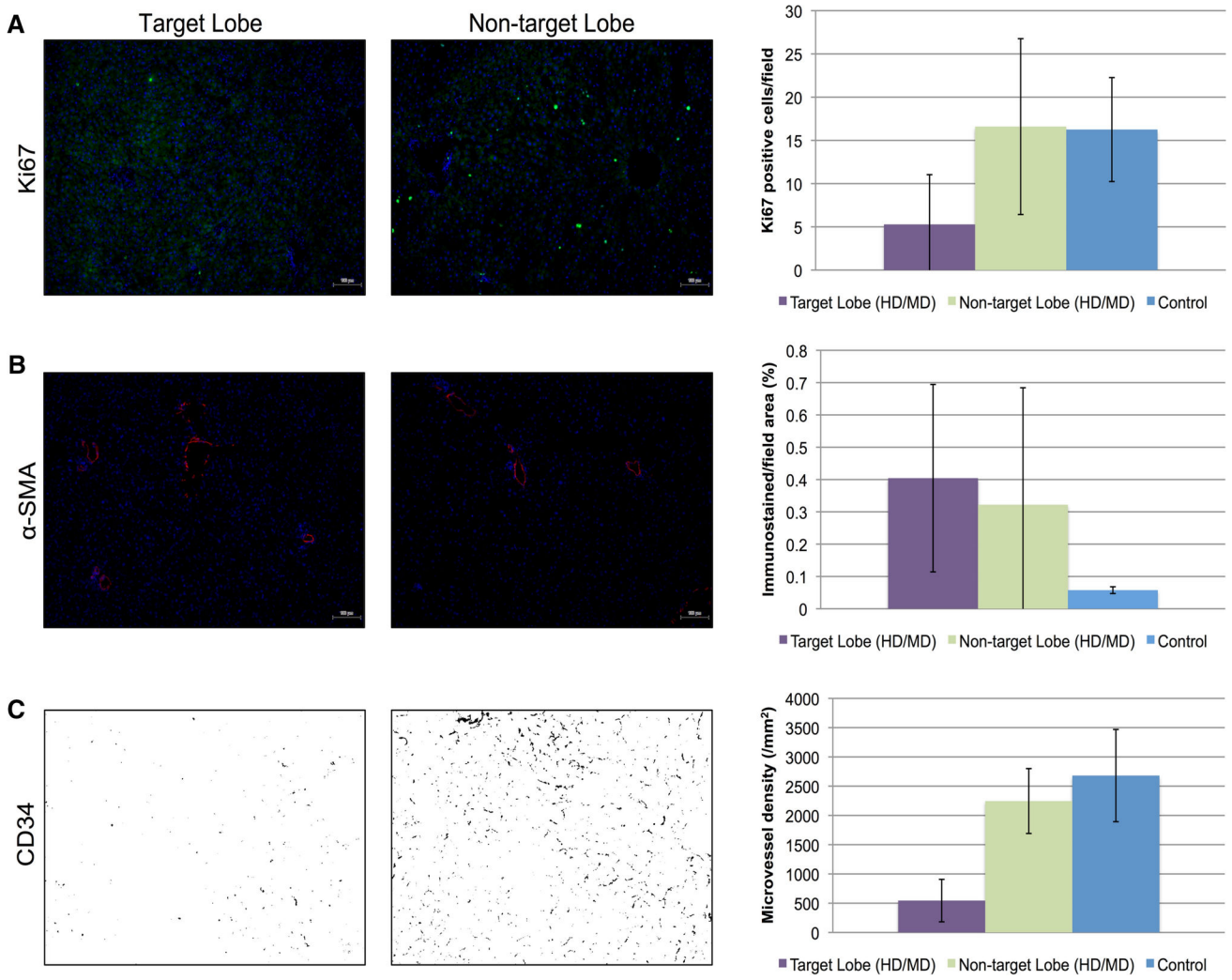

Figure 6.

Representative immunofluorescence results for (A) Ki67 (100x, green), (B) α-SMA (100x, red), and (C) CD34 staining (200x) in very high-, high- and medium-dose rats (HD/MD) (n=8) and untreated controls (n=2). Scale bar = 100 μm. The target (RML, purple) and non-target lobe (LLL, green) were compared for Y90 PVE rats. High-/medium-dose irradiation of the target lobe was associated with a local decrease in hepatocyte proliferation and decreased microvessel density at 12 weeks. The area of positive α-SMA staining appeared similarly elevated for both the target and non-target lobes relative to controls.

Table 1.

Y-90 Activity by Group

Group	Planned Activity (MBq)	Administered Activity (MBq)	Residual Activity (%)
Very High (n=2)	241.6 ± 3.0	196.8 ± 14.1	18.5 ± 6.9
High (n=10)	79.6 ± 17.8	64.0 ± 16.3	19.8 ± 9.0
Medium (n=5)	52.9 ± 20.4	27.8 ± 4.4	40.9 ± 22.0
Low (n=5)	13.0 ± 3.3	6.3 ± 2.6	53.1 ± 10.7

Note. - Values are means ± SD.

Table 2.

Y-90 Microsphere Ex Vivo Distribution (n=4)

Location	Percent Total Activity (%)	Mass (g)	Relative Activity (MBq/g)*	Dose (Gy)*
Lung	1.2 ± 0.9%	3.15 ± 0.70	0.58 / 0.58 / 0.51 / 0.0	29.1 / 29.0 / 25.7 / 0.0
RML	93.8 ± 2.7%	2.86 ± 0.28	58.49 / 27.49 / 24.47 / 18.96	2924.5 / 1374.3 / 1223.4 / 948.1
LML	2.3 ± 1.3%	1.72 ± 0.67	3.16 / 1.20 / 0.57 / 0.75	158.2 / 59.7 / 28.3 / 37.4
LLL	0.9 ± 0.8%	4.32 ± 0.94	0.37 / 0.16 / 0.41 / 0.0	18.6 / 7.8 / 20.5 / 0.0
RLL	1.1 ± 1.1%	2.32 ± 0.76	0.68 / 1.18 / 0.44 / 0.0	33.9 / 59.3 / 22.1 / 0.0
CL	0.7 ± 0.8%	1.36 ± 0.33	2.04 / 0.94 / 0.0 / 0.0	101.8 / 47.1 / 0.0 / 0.0

Note. - Values are means ± SD.

*Each rat had a different vial activity and residual, therefore the MBq/g and calculated dose are reported for each individual case.

RML, right median lobe; LML, left median lobe; LLL, left lateral lobe; RLL, right lateral lobe; CL, caudate lobe.